Quantitative Error Analysis of Polarimetric Phased Array Radar Measurements

Junho Ho[1,2], Guifu Zhang[1,2], Zhe Li[3], Petar Bukovcic[4,5], Alexander Ryzhkov[4,5], Jidong Gao[5], Jacob T. Carlin[4,5], and Jeffrey Snyder[5]

[1]School of Meteorology, University of Oklahoma, Norman, OK, U.S.A. [2]Advanced Radar Research Center, University of Oklahoma, Norman, OK, U.S.A.
[3]MathWorks, Natick, Massachusetts, U.S.A.
[4]Cooperative Institute for Severe and High-Impact Weather Research and Operations, University of Oklahoma, Norman, OK, U.S.A.
[5]NOAA/OAR National Severe Storms Laboratory, Norman, OK, U.S.A.

Email: jhho0626@ou.edu

Introduction

- The S-band fully digital planar polarimetric phased array radar (PPPAR), named Horus, was developed by the Advanced Radar Research Center at the University of Oklahoma (OU) with funding from the National Severe Storms Laboratory (NSSL) and the Office of Naval Research (Palmer et al., 2023).
- The fully digital design provides numerous advantages, including high flexibility in spatio-temporal resolution and sampling, beam agility, interference mitigation, and, in theory, software configurability.
- However, as a 2D PPPAR, Horus faces challenges in calibrating polarimetric variables to meet the requirements of weather observation (Zhang et al., 2009; Zhang et al., 2011; Palmer et al., 2023).

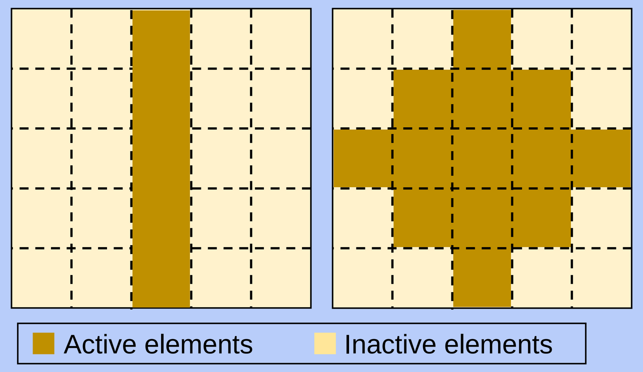

Figure 1. Depiction of the active elements used for 5- and 13-panel measurements. The dark yellow denotes the active elements, and the lighter yellow inactive.

Table 1. Specifications relevant to the sensitivity of 5- and 13-panel Horus, and KTLX

Radar Parameters	5-panel Horus	13-panel Horus	KTLX
Frequency (GHz)	3.07	3.07	2.8
Transmit power (kW/polarization)	3.2	8.32	375
Antenna gain (dB)	26.5	31.5	45.5
Elevation beamwidth (°)	3.3	3.3	0.925
Azimuth beamwidth (°)	13	3.3	0.925

Objectives of this study:

- Analyze the error statistics of the weather observations.
- Assess the quality of the polarimetric data in its current state and locate potential system deficiencies.
- Guide further system development and post processing techniques for meteorological applications.

Comparison with WSR-88D

- The reconstructed range-height indicator (RHI) from KTLX, a nearby operational WSR-88D radar, was used as a reference to quantify the mean bias of Horus measurements.

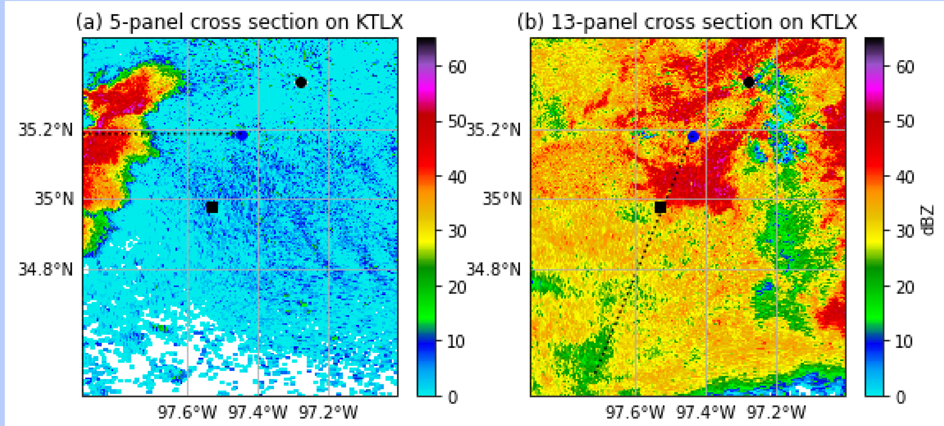

Figure 2. Plot of observed reflectivity (Z_H) from KTLX for regions of Horus with 5 panel (left) and 13 panel (right) weather measurements at 23:44 UTC on 11 May 2023 and 22:39 UTC 4 October 2023, respectively. The blue circle denote Horus, the black circle denotes KTLX, and the black square denotes the two-dimensional video disdrometer.

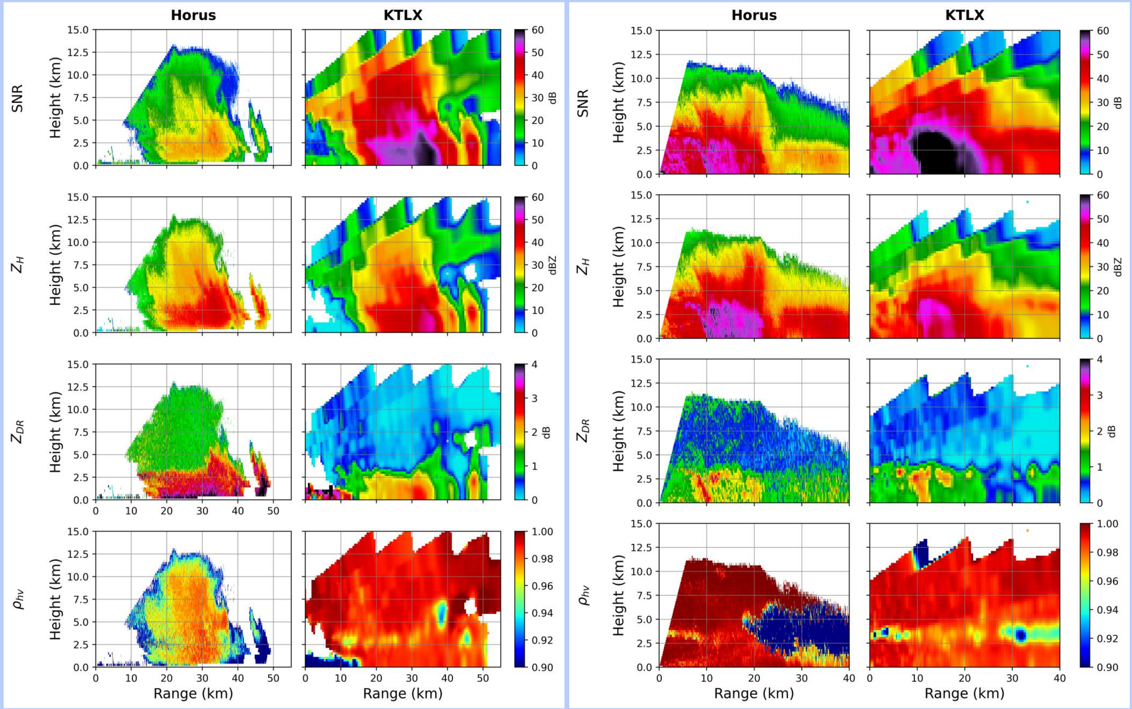

Figure 3. Spatial distribution of SNR, Z_H, Z_{DR}, and ρ_{hv} from Horus and KTLX measurements. The polarimetric variables are plotted for SNR larger than 10 dB. The plots on the left are based on 5-panels, and right 13-panels.

- In Figure 3 and Table 2, we demonstrate
  - both the 5- and 13-panel observations matched well with the nearby operational dish-based KTLX.
  - Horus shows more detailed microphysical and dynamical processes owing to higher spatiotemporal resolution.
  - Relatively higher Z_{DR} and ρ_{hv} biases are noticed far off-broadside, and in lower elevations due to ground clutter contamination.
  - The influence of beam mismatch is limited, and the results accurately reflect the biases of the current system in weather observations.
- Further investigation into the persistently negative ρ_{hv} appears to be necessary.

	0≤SNR	5≤SNR	10≤SNR	15≤SNR	20≤SNR
Z_H (dBZ)	4.46 (4.17)	4.46 (4.17)	4.66 (4.39)	4.99 (4.76)	5.45 (5.13)
Z_{DR} (dB)	0.28 (0.30)	0.28 (0.30)	0.27 (0.29)	0.26 (0.28)	0.25 (0.27)
ρ_{hv}	−0.009 (0.006)	−0.009 (0.006)	−0.01 (0.006)	−0.011 (0.006)	−0.009 (0.006)

Table 2. Table of the mean biases for the differences between Horus and KTLX for each signal-to-noise ratio (SNR) range.

Error statistics

- **Bias**
  - The reconstructed KTLX RHI was formed over the Horus measurement plane for comparison.
  - To ensure accurate comparison, each elevation and time were carefully matched by selecting the Horus rays from the best-matching KTLX observation time for each elevation angle.
  - The KTLX reconstructed RHI and Horus RHI scans were both interpolated to 10-m horizontal and 125-m vertical grids.
- **Standard deviation**
  - **Spatial samples**

    As demonstrated in an earlier CPPAR data analysis (Li et al., 2021), 11 consecutive range gates were employed as shown,

$$\mathrm{STD}(X) = \sqrt{\frac{1}{11}\sum_{m=i-5}^{i+5}(X_m - \bar{X})^2}$$

i the gate number;
X_m the polarimetric data at gate m;
$\bar{X}$ the mean value of consecutive 11 gates.

  - **Temporal samples**
    - Horus data provide rapid updates every 2 to 4 seconds, enabling the computation of the standard deviation of radar data from temporal samples given the assumptions of ergodicity and local stationarity
    - The 127 temporal samples selected after removing abnormal time steps/stripes were used to calculate the standard deviation using

$$\mathrm{STD}(X) = \sqrt{\frac{1}{2(N-1)}\sum_{n=1}^{N-1}|(X_{n+1} - X_n)|^2}$$

N the number of temporal samples;
X_{n+1} the polarimetric variables at t_{n+1};
X_n the polarimetric variables at t_n.

Standard deviation from spatial and temporal samples

- Table 3 and Figure 4 display the calculated standard deviations for each signal-to-noise ratio (SNR) range, theoretical values, and the NOAA/NWS radar functional requirements (RFR), based on spatial and temporal sampling.
- The standard deviations from spatial samples exhibit lower values than those from temporal samples and theory due to the influence of spatial averaging and smoothing techniques.
- The ground clutter effect, coupled with the use of a progressive pulse compression technique to remove the blind range, result in higher standard deviations at lower elevations and up to 12 km in range (Salazar Aquino et al., 2021).
- The higher standard deviation stripes in Z_{DR} and ρ_{hv} are associated with the combination of non-uniform beamfilling and steering far off-broadside .

(a) Spatial

	0≤SNR	5≤SNR<10	10≤SNR<15	15≤SNR<20	20≤SNR	Theory	NOAA/NWS RFR
Z_H (dBZ)	1.31	0.62	0.87	0.63	**1.31**	1.31	1.8
v_r (m/s)	0.41	0.43	0.39	0.31	**0.39**	0.46	1.0
σ_v (m/s)	0.41	0.53	0.38	0.30	**0.39**	0.31	1.0
Z_{DR} (dB)	0.09	0.12	0.08	0.06	**0.08**	0.17	0.3
ρ_{hv}	0.002	0.014	0.006	0.002	**0.001**	0.001	0.006
Φ_{DP} (°)	0.93	1.33	0.92	0.65	**0.84**	1.11	2.0

(b) Temporal

	0≤SNR	5≤SNR<10	10≤SNR<15	15≤SNR<20	20≤SNR	Theory	NOAA/NWS RFR
Z_H (dBZ)	1.74	0.94	1.00	0.98	**1.82**	1.31	1.8
v_r (m/s)	0.53	0.74	0.59	0.57	**0.51**	0.46	1.0
σ_v (m/s)	0.54	0.81	0.54	0.46	**0.52**	0.31	1.0
Z_{DR} (dB)	0.20	0.34	0.23	0.16	**0.17**	0.17	0.3
ρ_{hv}	0.005	0.030	0.015	0.006	**0.003**	0.001	0.006
Φ_{DP} (°)	1.68	3.08	2.07	1.51	**1.40**	1.11	2.0

Table 3. The standard deviation of six moments based on both (a) the spatial and (b) the temporal domain of the Horus data for five different signal-to-noise ratio (SNR) ranges. The NOAA/NWS RFR represents the radar functional requirements of the NOAA and National Weather Service. The results are based on 13-panel measurements.

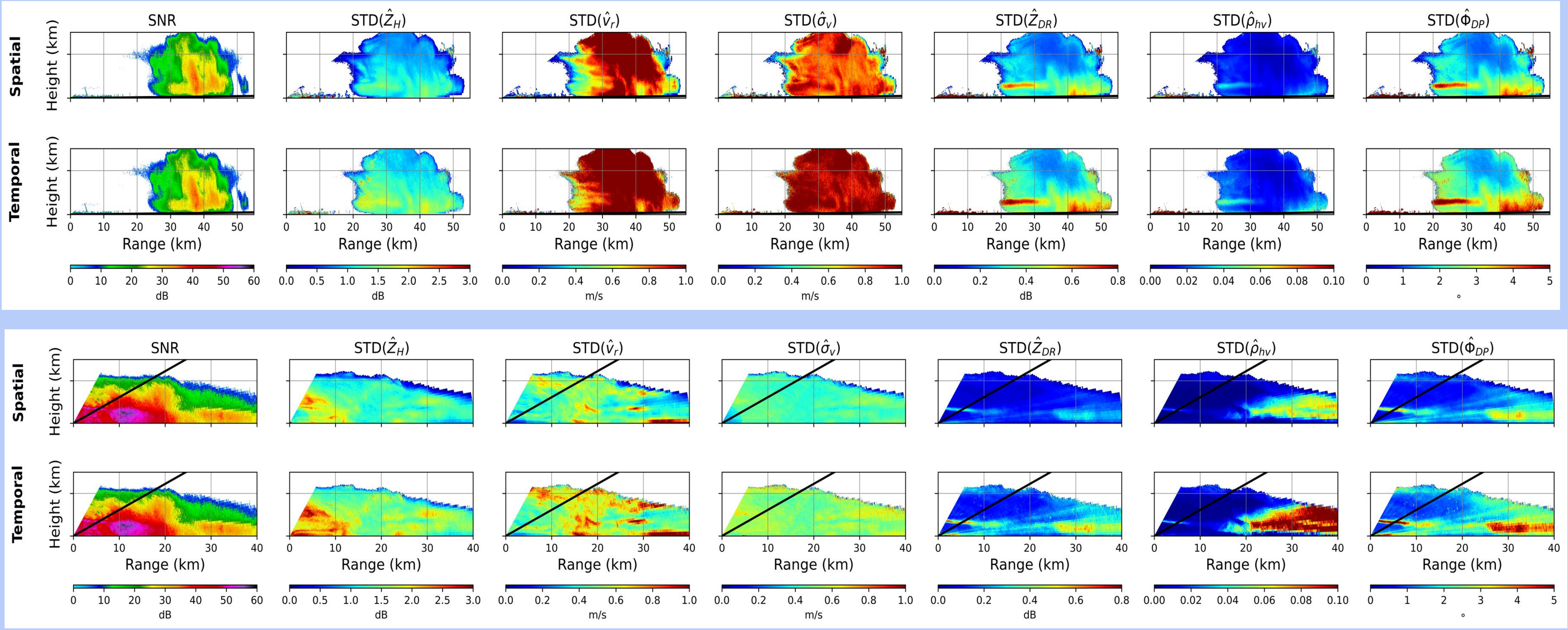

Figure 4. Spatial distribution of SNR, and standard deviations of reflectivity (Z_H), radial velocity (v_r), spectrum width (σ_v), differential reflectivity (Z_{DR}), correlation coefficient (ρ_{hv}), and differential phase shift (Φ_{DP}) for SNR larger than 10 dB from Horus weather observations based on 127 timesteps on 04 October 2023. The first row utilizes 11 spatial gates, and the second row only temporal samples. The top plot is based on 5-panels, and bottom 13-panels. The black solid lines denote the broadside.

Summary

- The polarimetric data quality of measurements from Horus, a 2D electronically scanning PPPAR, were analyzed.
- The mean differences and standard deviation of Horus with 5 panels and 13 panels were compared with those of a collocated operational radar. Both measurements from 5-and 13-panels matched well.
- The standard deviations using spatial and temporal samples were calculated; the radar variables from both number of panels agree well with theory and fit within the NOAA/NWS RFR for the cases examined.
- Stripes of higher standard deviation in polarimetric variables and negatively biased ρ_{hv} off-broadside are noticed.
- Further advancements in the Horus's design and calibration methods are in progress, and the issues identified in this study will likely be solved in the future.

AMERICAN METEOROLOGICAL SOCIETY
AMS 2024
104TH ANNUAL MEETING
28 JANUARY-1 FEBRUARY 2024
BALTIMORE, MD & ONLINE

POSTER ID
438751

Reference

1. Palmer, R. D., et al., IEEE Trans. on Radar Systems (2023)
2. Zhang, G., et al., IEEE Trans. On Geosci. and Remote Sens. (2009)
3. Zhang, G., et al., J. Atmos. and Oceanic Tech. (2011)
4. Li, Z.,, et al., IEEE Geosci. and Remote Sens. Letters (2021)
5. Salazar Aquino, C. M., et al., J. Atmos. And Oceanic Tech., (2021)

Acknowledgement

This work is partially supported by the National Oceanic and Atmospheric Administration (NOAA) under Grant NA16OAR4320115 and the National Science Foundation with the grant of AGS-2136161.